

Frame-wise distortion correction in Multi-echo Echo Planar Imaging

Andrew N. Van^{1,2}, M. Dylan Tisdall³, Timothy O. Laumann⁴, David F. Montez^{2,4}, Damien A. Fair^{5,6,7}, and Nico U.F. Dosenbach^{1,2,8,9}

¹Department of Biomedical Engineering, Washington University in St. Louis, St. Louis, MO, United States, ²Department of Neurology, Washington University School of Medicine, St. Louis, MO, United States, ³Department of Radiology, Perelman School of Medicine, University of Pennsylvania, Philadelphia, PA, United States, ⁴Department of Psychiatry, Washington University School of Medicine, St. Louis, MO, United States, ⁵Institute of Child Development, University of Minnesota Medical School, Minneapolis, MN, United States, ⁶Department of Pediatrics, University of Minnesota Medical School, Minneapolis, MN, United States, ⁷Masonic Institute for the Developing Brain, University of Minnesota Medical School, Minneapolis, MN, United States, ⁸Department of Radiology, Washington University School of Medicine, St. Louis, MO, United States, ⁹Department of Pediatrics, Washington University School of Medicine, St. Louis, MO, United States

Synopsis

Echo Planar Imaging (EPI) suffers from off-resonance image distortion due to B0 inhomogeneities. These distortions are typically corrected by separate field map acquisitions, but only allow for sparse temporal sampling of B0 inhomogeneity. This approach prevents distortion correction if changes in the B0 field occur over time due to motion. Here, we present a method of correcting off-resonance distortion by computing a time series of field maps using phase information from multi-echo (ME) EPI data. We show that our method produces corrections comparable to the current standard of distortion correction, in addition to enabling frame-by-frame correction in functional MRI data.

Purpose

Multi-echo Echo Planar Imaging (ME-EPI) acquires multiple images along the T2* decay of the free-induction decay signal, with each image centered around a different echo time. In the context of functional neuroimaging, these echo measurements have been used to improve detection of the BOLD signal and reduce artifacts in functional MRI (fMRI) data¹⁻³. However, ME-EPI, like all EPI acquisitions, suffer from off-resonance image distortion due to inhomogeneities in the B0 field. At present, these distortions are corrected using separate field map acquisitions that measure and enable the correction of B0 inhomogeneities^{4,5}. However, current field map acquisition methods only allow for the measurement of B0 inhomogeneities at a single point in time, and can only be measured at the beginning and/or end of an fMRI block. Thus, B0 field inhomogeneities are mostly unknown during the fMRI acquisition, and may vary as participants move. Here, we present a method of B0 inhomogeneity measurement and distortion correction in ME-EPI on a frame-by-frame basis that does not require additional scanning time.

Methods

Magnitude and phase ME-EPI data (TR: 1.761 s, TEs: 14.2, 38.93, 63.66, 88.39, 113.12 ms, 72 Slices, FOV: 110x110, Voxel Size: 2.0 mm, Multi-Band: 6) was collected using a 3T whole-body scanner (Prisma, Siemens Healthcare) from a participant with minimal head motion and another participant with frequent head motion. For each TR, phase images from each echo were unwrapped and a field map was calculated using the ROMEO phase unwrapping tool⁶. Each computed field map was brain masked and converted into a displacement field by multiplying the field map by the effective echo spacing, number of phase encoding lines, and the voxel size⁷. The displacement field was then inverted and used to unwarp each frame of the ME-EPI data using Advanced Normalization Tools (ANTs)⁸. For a ground truth comparison, reverse phase-encoded (RPE) spin-echo EPI images (TR: 8 s, TE: 66 ms, 72 Slices, FOV: 110x110, Voxel Size: 2.0mm) were acquired to obtain a ground truth field map using FSL topup⁵. Additional T1w (Multiecho MPRAGE, TR: 2.5 s, TEs: 1.81, 3.6, 5.39, 7.18 ms, 208 Slices, FOV: 300x300, Voxel Size: 0.8 mm, Bandwidth: 745 Hz/px) and T2w (T2 SPACE, TR: 3.2, TE: 565 ms, 176 Slices, Turbo Factor: 190, FOV: 256x256, Voxel Size: 1 mm, Bandwidth: 240 Hz/px) anatomical scans were collected to compare distortion correction accuracy by assessing the correspondence between the functional data to the anatomy. The ME field map was compared to the RPE field map, by extracting the first frame of the ME field maps, smoothing the ME field map with a Gaussian kernel (FWHM 4 mm), then calculating the difference between the ME field map and the RPE field map. The reliability of ME field map measurement and phase unwrapping was measured through a frame-to-frame correlation coefficient computation between each field map. Distortion correction accuracy was assessed by overlaying T1w/T2w-derived anatomical segmentation computed by FreeSurfer before any correction, after RPE correction, and after ME correction⁹. Finally, field map differences were assessed in a subject with large frame-to-frame motion, by computing the field maps in each frame and co-registering the field maps with a rigid-body transform¹⁰.

Results

Comparison of field maps obtained from ME-fMRI data and RPE method are visualized in Figure 1. Field maps computed from ME phase data are visually similar to field maps computed from the RPE method. Frame-to-frame field map solutions are visualized in Figure 2, and are highly reliable ($R = 0.961 \pm 0.0244$). Geometry of the 1st echo of ME-fMRI data is compared to the anatomical segmentation before/after correction in Figure 3. Distortion correction with ME field map improves correspondence to anatomical gray/white matter boundaries. Field maps from a participant with large motion between two frames are compared in Figure 4. Head motion parameters between the two frames were $\Delta x = -1.959$ mm, $\Delta y = 1.172$ mm, $\Delta z = -1.589$ mm, $r_x = 2.092^\circ$, $r_y = 0.918^\circ$, $r_z = 0.745^\circ$ and framewise displacement (FD) 7.997 mm.

Discussion

Our results show field maps obtained from phase images of ME-EPI data are comparable to those obtained from current gold standard methods (i.e. RPE field maps). Large differences in the ME field map, with respect to the RPE field maps, are localized to areas of significant signal loss between echoes, preventing accurate phase measurement. However, this did not seem to affect overall distortion correction quality. Another concern relates to the accuracy of phase unwrapping due to the relatively echo long time differences, which can lead to highly wrapped phase images at longer echo times and prevent accurate field map computation. Despite this challenge, phase unwrapping with ROMEO yielded consistent results as evidenced by the highly reliable field map solutions from each TR of fMRI data. In subjects with large frame-to-frame motion, our method is able to compute field map changes due to differences in head position. These preliminary results show field maps derived from multi-echo phase data can produce an accurate time-series of field maps for frame-by-frame distortion correction. This will obviate the need for separate field map acquisitions and enable motion-robust distortion correction in ME-EPI data, improving overall data quality for functional neuroimaging experiments.

Acknowledgements

No acknowledgement found.

References

1. Kundu P, Voon V, Balchandani P, Lombardo MV, Poser BA, Bandettini PA. Multi-echo fMRI: A review of applications in fMRI denoising and analysis of BOLD signals. *NeuroImage*. 2017 Jul 1;154:59–80.
2. Steel A, Garcia BD, Silson EH, Robertson CE. Evaluating the efficacy of multi-echo ICA denoising on model-based fMRI. *NeuroImage*. 2022 Dec 1;264:119723.
3. DuPre E, Salo T, Ahmed Z, Bandettini PA, Bottenhorn KL, Caballero-Gaudes C, Dowdle LT, Gonzalez-Castillo J, Heunis S, Kundu P, Laird AR, Markello R, Markiewicz CJ, Moia S, Staden I, Teves JB, Uruñuela E, Vaziri-Pashkam M, Whitaker K, Handwerker DA. TE-dependent analysis of multi-echo fMRI with *tedana*. *Journal of Open Source Software*. 2021 Oct 12;6(66):3669.
4. Jezzard P, Balaban RS. Correction for geometric distortion in echo planar images from B0 field variations. *Magnetic Resonance in Medicine*. 1995;34(1):65–73.
5. Andersson JLR, Skare S, Ashburner J. How to correct susceptibility distortions in spin-echo echo-planar images: application to diffusion tensor imaging. *NeuroImage*. 2003 Oct 1;20(2):870–888.
6. Dymerska B, Eckstein K, Bachrata B, Siow B, Trattinig S, Shmueli K, Robinson SD. Phase unwrapping with a rapid opensource minimum spanning tree algorithm (ROME0). *Magnetic Resonance in Medicine*. 2021;85(4):2294–2308.
7. Smith SM. Fast robust automated brain extraction. *Hum Brain Mapp*. 2002 Nov;17(3):143–155. PMID: PMC6871816
8. Avants BB, Epstein CL, Grossman M, Gee JC. Symmetric diffeomorphic image registration with cross-correlation: Evaluating automated labeling of elderly and neurodegenerative brain. *Medical Image Analysis*. 2008 Feb 1;12(1):26–41.
9. Dale AM, Fischl B, Sereno MI. Cortical Surface-Based Analysis: I. Segmentation and Surface Reconstruction. *NeuroImage*. 1999 Feb 1;9(2):179–194.
10. Jenkinson M, Bannister P, Brady M, Smith S. Improved Optimization for the Robust and Accurate Linear Registration and Motion Correction of Brain Images. *NeuroImage*. 2002 Oct;17(2):825–841.

Figures

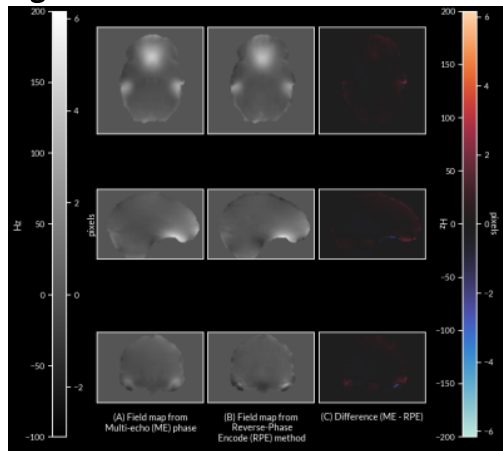


Figure 1: (A) Field map computed from phase of ME-fMRI data, (B) field map computed from RPE method, and (C) difference between the two field maps (ME - RPE).

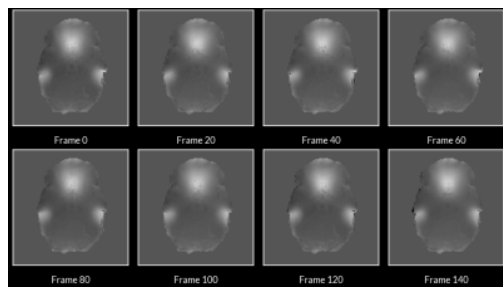


Figure 2: Field maps computed at each frame of the ME-EPI data. Frame-to-frame field maps solutions were highly consistent ($R = 0.961 \pm 0.0244$).

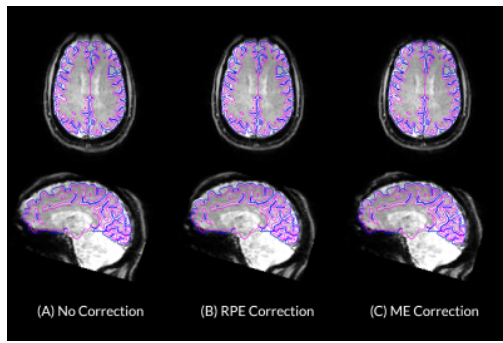


Figure 3: Transverse and Sagittal views of ME-fMRI reference data (A) ME-fMRI data before distortion correction, (B) after correction with field map computed from RPE method, and (C) after correction with field map obtained from ME-fMRI phase data. Blue and fuchsia borders represent anatomical pial and white matter surfaces respectively. Surfaces were derived from anatomical segmentations computed by FreeSurfer.

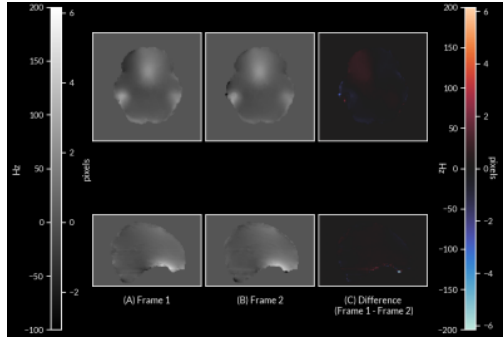


Figure 4: Co-registered field maps from two frames of high motion subject (head motion parameters: $\Delta x = -1.959$ mm, $\Delta y = 1.172$ mm, $\Delta z = -1.589$ mm, $r_x = 2.092^\circ$, $r_y = 0.918^\circ$, $r_z = 0.745^\circ$; FD = 7.997 mm) (A) field map from first frame (B) field map from second frame (C) difference of field map between the two frames due to head motion.